# Test of supersymmetry in $e^-e^-$ collisions

W.-Y. Keung and L. Littenberg
*Physics Department, Brookhaven National Laboratory, Upton, New York 11973*
(Received 9 March 1983)

The production of scalar electrons in $e^-e^-$ collisions can proceed by exchange of a Majorana fermion, which is the photino in supersymmetric theories. Detection of this process will establish the self-conjugate nature of the photino and thus serve as a test of supersymmetry. Reactions of particular polarization configurations $e_L^-e_L^-$ or $e_R^-e_R^-$ are sensitive to the photino mass. We study the predicted cross sections and the event distributions.

## I. INTRODUCTION

Supersymmetry, if valid, requires a proliferation of particles, namely, supersymmetric partners of ordinary particles, e.g., scalar leptons, scalar quarks, photinos, gluinos etc. One purpose of introducing supersymmetry is to solve the hierarchy problem of grand unified models. This solution[1] requires the supersymmetric partners of known particles to lie below 1 TeV, and probably within the reach of the next generation of accelerators.

Much work on the phenomenology[2] of the supersymmetry has been done for $e^+e^-$,[3] $pp$, or $\bar{p}p$ collisions.[4] Here we raise some questions. If new thresholds are crossed and unusual events are observed, will they provide unambiguous evidence of supersymmetry? Are there ways to test the self-conjugate nature of the photino? Of course, the event topology can help to answer these questions,[3] but it will not be simple and clean due to the complication introduced by the decay patterns of the new particles and to the presence of backgrounds.

In this paper, we study scalar-electron production in $e^-e^-$ collisions via a photino-exchange mechanism. The observation of such events can quite definitely establish the properties of self-conjugation of the photino and thus serve as a test of supersymmetry. In Sec. II, the process $e^-e^-\rightarrow$ scalar electrons is described and the relevant amplitudes given. The resulting cross-section formulas are presented and discussed. Section III discusses the general features and the phenomenology of these production mechanisms.

## II. CROSS-SECTION FORMULAS

In supersymmetric models, the right-handed and left-handed chiralities of the electron are associated with a pair of scalar partners, $t_e$ and $s_e$, respectively. Likewise, the photon has its own Majorana-fermion partner, the $\tilde{\gamma}$ photino. The relevant interaction among $t_e$, $s_e$, $e$, and $\tilde{\gamma}$, as required by supersymmetry, is

$$\mathcal{L}_{\rm int}=-\sqrt{2}(\bar{e}_R t_e+\bar{e}_L s_e)\tilde{\gamma}+\text{H.c.} \tag{1}$$

Supersymmetry breaking, whether spontaneous or soft and explicit, generates large masses for $t_e$ and $s_e$. We assume for simplicity, as also suggested by most models, that $t_e$ and $s_e$ are degenerate in mass and that $\tilde{m}_e \gg m_e$.

The production of a pair of scalars $i$ and $j$ ($i,j=t_e$ or $s_e$) in the $e^-e^-$ collision proceeds by the photino exchange. Let $p_1,p_2$ be the initial electron momenta and $k_i,k_j$ be the momenta of the outgoing scalar electrons of types $i$ and $j$. The overall amplitude is

$$\mathcal{M}=2ie^2\bar{v}(p_2)\Gamma_j\frac{\not{p}_1-\not{k}_i+\tilde{m}_\gamma}{(p_1-k_i)^2-\tilde{m}_\gamma{}^2}\Gamma_i u(p_1)-(1\leftrightarrow 2)\ . \tag{2}$$

Here $\Gamma_{s_e}=(1-\gamma_5)/2$ and $\Gamma_{t_e}=(1+\gamma_5)/2$. The second term in Eq. (2) comes from the antisymmetrization of the amplitude due to the Fermi statistics of the electron. In the calculation, the use of the charge-conjugation matrix $C$ allows the $\bar{v}u$ ordering in the second term to be the same as that in the first term. It is straightforward to see that the amplitudes for $e^-e^-\rightarrow s_e s_e$ or $t_e t_e$ vanish for the case of a massless photino $\tilde{m}_\gamma=0$. However, the amplitude for $e^-e^-\rightarrow s_e t_e$ is nonvanishing. Our calculation neglects the electron mass. The effect of the Goldstone-fermion interaction has also been ignored. For each channel, we obtain the differential cross sections in terms of the usual Mandelstam variables for arbitrary photino mass,

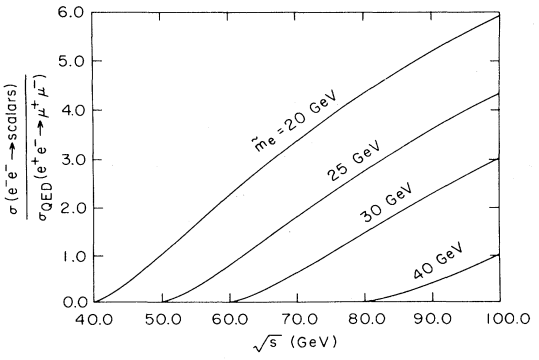


FIG. 1. The total cross section for $e^-e^-\rightarrow$ scalar electrons versus $\sqrt{s}$ for different cases $\tilde{m}_e=20$, 25, 30, or 40 GeV, assuming a massless photino.

 

$$d\sigma(e_L^- e_R^- \to s_e t_e)/dt = 4\pi\alpha^2 s^{-2}(ut - \tilde{m}_e^4)(t - \tilde{m}_\gamma^2)^{-2} , \tag{3}$$

$$d\sigma(e_R^- e_L^- \to s_e t_e)/dt = 4\pi\alpha^2 s^{-2}(ut - \tilde{m}_e^4)(u - \tilde{m}_\gamma^2)^{-2} . \tag{4}$$

$$d\sigma(e_L^- e_L^- \to s_e s_e)/dt = d\sigma(e_R^- e_R^- \to t_e t_e)/dt = (1/2!)4\pi\alpha^2 s^{-1}\tilde{m}_\gamma^2[(t - \tilde{m}_\gamma^2)^{-1} + (u - \tilde{m}_\gamma^2)^{-1}]^2 . \tag{5}$$

The statistical factor (1/2!) in Eq. (5) stems from the identical particles in the final state. Summing over all channels, the differential cross section for the unpolarized beams is

$$d\sigma/dt = \pi\alpha^2 s^{-2}\{(ut - \tilde{m}_e^4)[(t - \tilde{m}_\gamma^2)^{-2} + (u - \tilde{m}_\gamma^2)^{-2}] + s\tilde{m}_\gamma^2[(t - \tilde{m}_\gamma^2)^{-1} + (u - \tilde{m}_\gamma^2)^{-1}]^2\} . \tag{6}$$

The corresponding integrated cross sections are listed below:

$$\sigma(e_L^- e_R^-) = \frac{4\pi\alpha^2}{s}\left[\frac{1+\beta^2+\delta}{2}\ln\frac{(1+\beta)^2+\delta}{(1-\beta)^2+\delta} - 2\beta\right] , \tag{7}$$

$$\sigma(e_R^- e_L^-) = \sigma(e_L^- e_R^-) , \tag{8}$$

$$\sigma(e_L^- e_L^-) = \frac{4\pi\alpha^2}{s}\delta\left[\frac{1}{1+\beta^2+\delta}\ln\frac{(1+\beta)^2+\delta}{(1-\beta)^2+\delta} + \frac{4\beta}{(1+\beta^2+\delta)^2 - 4\beta^2}\right] , \tag{9}$$

$$\sigma(e_R^- e_R^-) = \sigma(e_L^- e_L^-) \tag{10}$$

with $\beta^2 = 1 - 4\tilde{m}_e^2/s$ and $\delta = 4\tilde{m}_\gamma^2/s$. The total cross section for the unpolarized beams is

$$\sigma = \tfrac{1}{2}[\sigma(e_L^- e_R^-) + \sigma(e_L^- e_L^-)] . \tag{11}$$

After production, the scalar electrons decay with an extremely short life time into an electron and a photino (if kinematics allow) or a Goldstone fermion. Since the photino or Goldstone fermion rarely interacts[5] with the material of the detector, the observed final configuration consists of noncoplanar $e^- e^-$ with, on the average, half the energy missing in the undetected neutrals.

## III. CROSS-SECTION RESULTS

Figure 1 shows the total cross section for $e^- e^- \to$ scalar electrons versus $\sqrt{s}$ for different cases $\tilde{m}_e = 20$, 25, 30, or 40 GeV, assuming a massless photino. The rates are normalized to the pure QED prediction for $\sigma_{\rm QED}(e^+ e^- \to \mu^+ \mu^-)$, which is usually denoted as one unit of $R$,

$$\sigma_{\rm QED}(e^+ e^- \to \mu^+ \mu^-) = 4\pi\alpha^2/3s \approx 87 \text{ nb}(1 \text{ GeV}^2/s) . \tag{12}$$

At the proposed Stanford Linear Collider (SLC) energies[6] of around 100 GeV, several units of $R$ for $\sigma(e^- e^- \to$ scalar electrons) are expected if $\tilde{m}_e$ is around 30 GeV. The cross section rises with energy due to the $t$-pole enhancement.

Figure 2 shows the effect of the photino mass upon the cross section. Near the threshold, a larger production rate occurs for a nonvanishing photino mass. This behavior stems from the fact that the channels $e^- e^- \to s_e s_e$ or $t_e t_e$ are reopened for a finite $\tilde{m}_\gamma$.

From an experimental point of view, it is important to note that although the $t$-channel pole leads to forward-

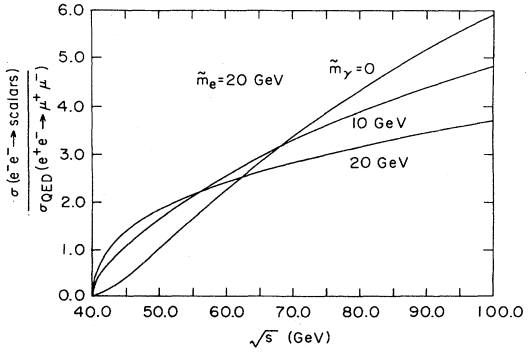


FIG. 2. Effect of the photino mass upon the cross sections. The cases $\tilde{m}_\gamma = 0$, 10, and 20 GeV with $\tilde{m}_e = 20$ GeV are illustrated.

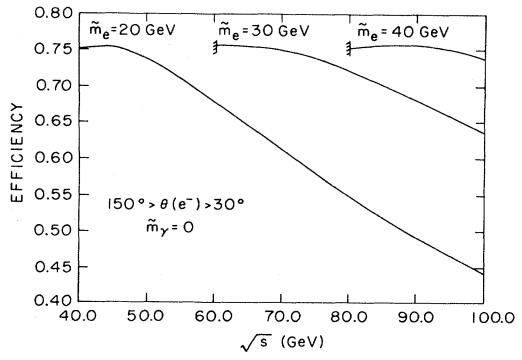


FIG. 3. Detection efficiency versus $\sqrt{s}$ for fiducial area cuts $30° < \theta(e^-) < 150°$.

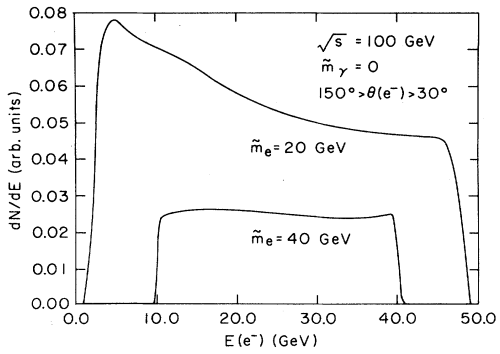


FIG. 4. The daughter-electron energy spectrum for $\tilde{m}_e = 20$ and 40 GeV at $\sqrt{s} = 100$ GeV.

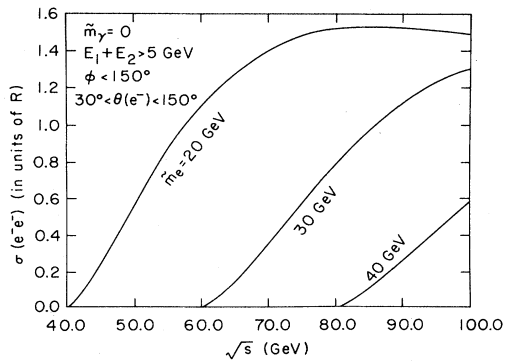


FIG. 6. Production rates for $\tilde{m}_e = 20$, 30, and 40 GeV versus $\sqrt{s}$ for the cut set $30° < \theta(e^-) < 150°$, $\phi < 150°$, and $E_1 + E_2 > 5$ GeV.

backward peaking in the scalar electron angular distribution, the decay electrons pick up considerable transverse momentum and quite frequently emerge at a large angle with respect to the beam. If one imposes fiducial-area cuts of $30° < \theta(e^-) < 150°$, roughly similar to those used in recent searches for scalar electrons in $e^+e^-$ collisions,[7] the resulting detection efficiencies are shown in Fig. 3. Typical efficiencies are 50% and are relatively gentle functions of $\sqrt{s}$, particularly for $\tilde{m}_e \gtrsim 30$ GeV. Thus in the results that follow we impose the $30° < \theta(e^-) < 150°$ cut.

Figure 4 shows the daughter-electron energy spectrum for $\tilde{m}_e = 20$ or 40 GeV at $\sqrt{s} = 100$ GeV. It is clear that a cut of $E_1 + E_2 \gtrsim 5$ GeV, as has been used[7] to reject the two-photon background in the $e^+e^-$ case, would have a very small effect on the scalar-electron signal. Another cut, which it has proved neccessary to make in the $e^+e^-$ case, is one in the azimuthal angle $\phi$ between the observed electrons. In lowest order, QED processes give $\phi = 180°$. Typically, one demands $\phi < 150°$. Figure 5 gives the $\phi$ distribution for $\tilde{m}_e = 20$ GeV at $\sqrt{s} = 100$ GeV. Although the distribution peaks at 180°, a cut at 150° is not disastrous, leading to a reduction in signal of about 40%. Figure 6 shows the rates for $\tilde{m}_e = 20$, 30, 40 GeV versus $\sqrt{s}$ for the cut set $30° < \theta(e^-) < 150°$, $\phi < 150°$, and $E_1 + E_2 > 5$ GeV. Assuming a conservative luminosity of $10^{30}$ cm$^{-2}$ sec$^{-1}$, one obtains about 0.75 events each day per unit of $R$ observed. Assuming that one can detect a signal of 10 events, at $\sqrt{s} = 100$ GeV, one can probe $\tilde{m}_e$ up to 46 GeV in a 100-day run. The mass of the scalar electron, $\tilde{m}_e$, can be measured directly from the threshold dependence of the cross section. If the $e^-e^-$ collider energy is fixed above the threshold, it is also possible to determine $\tilde{m}_e$ from event distributions,[3] provided that there is little background (for example, see Fig. 4).

It should be noted that several other properties of the scalar electron signal can also be exploited. Two examples are the given in Fig. 7 where the effective $e^-e^-$ mass and the missing mass recoiling against the electrons are plotted for the case $\tilde{m}_e = 20$ GeV at $\sqrt{s} = 100$ GeV. In principle, the latter could be exploited in vetoing QED backgrounds. However it is one of a number of kinematic quantities (another is the direction of the missing energy) whose usefulness would be enhanced by improving momentum resolution beyond that attained by current detectors.

Finally, it should be emphasized that polarized $e^-$ beams would represent an extremely powerful tool for the study of scalar-electron production. For example, in the likely event that the photino is quite light, because of the $\tilde{m}_\gamma^2/s$ suppression of Eq. (5), the scalar-electron signal

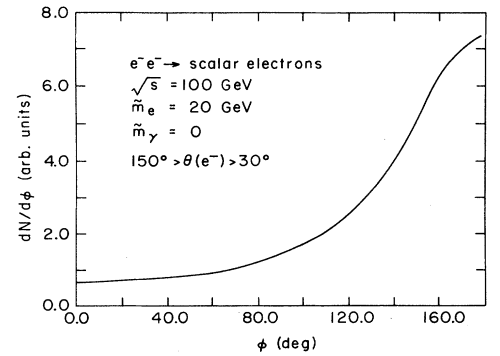


FIG. 5. The distribution of the azimuthal angle between the final electrons for the case $\tilde{m}_e = 20$ GeV at $\sqrt{s} = 100$ GeV.

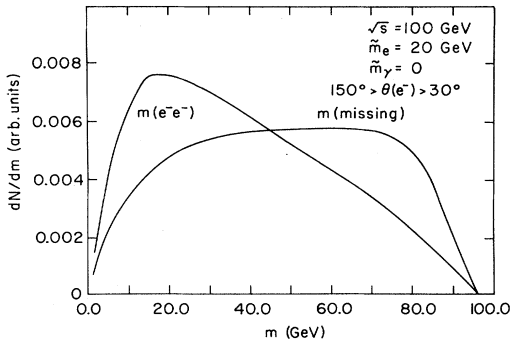


FIG. 7. The distributions of the invariant $e^-e^-$ mass and the missing mass for the case $\tilde{m}_e = 20$ GeV at $\sqrt{s} = 100$ GeV.

will be present only in $e_L^- e_R^-$ collisions. This is not at all true of competing processes (QED), other exotic-particle production, etc.). In the case of a massive photino, not only is the high-energy total cross section sensitive to $\tilde{m}_\gamma$ as shown in Fig. 2, but the ratio of $\sigma(e_L^- e_L^-)/\sigma(e_L^- e_R^-)$ can become large near threshold. For example, for $\tilde{m}_e = 20$, $\tilde{m}_\gamma = 10$ GeV at $\sqrt{s} = 50$ GeV, $\sigma(e_L^- e_R^-) = 1.3R$, and $\sigma(e_L^- e_L^-) = 2R$. Since the angular distributions are rather flat in this case, these effects should be readily observable.

## ACKNOWLEDGMENT

This work was supported by the U.S. Department of Energy under Contract No. DE-AC02-76CH0016.

[1]H. Georgi and S. Dimopoulos, Nucl. Phys. B193, 150 (1981); N. Sakai, Z. Phys. C 11, 153 (1982); E. Witten, Nucl. Phys. B188, 513 (1981).

[2]See review articles by I. Hinchliffe and L. Littenberg, in *Proceedings of the 1982 DPF Summer Study on Elementary Particle Physics and Future Facilities, Snowmass, Colorado,* edited by R. Donaldson, R. Gustafson, and F. Parge (Fermilab, Batavia, Illinois), p 242; P. Fayet, in *Proceedings of the 21st International Conference on High Energy Physics, Paris, 1982,* edited by P. Petiau and M. Pornuef [J. Phys. (Paris) Colloq. 43, (1982)].

[3]G. Farrar and P. Fayet, Phys. Lett. 89B, 191 (1980); P. Fayet, *ibid.* 117B, 460 (1982).

[4]G. Farrar and P. Fayet, Phys. Lett. 79B, 442 (1978); G. L. Kane and J. P. Leveille, Phys. Lett. 112B, 227 (1982); P. R. Harrison and C. H. Llewellyn Smith, Nucl. Phys. B213, 223 (1983).

[5]P. Fayet, Phys. Lett. 86B, 272 (1979).

[6]See SLC design reports, e.g., Proceedings of SLC Workshop on Experimental Use of Linear Collider, SLAC Report No. 247, 1982.

[7]H. Behrend *et al.* (CELLO Collaboration), Phys. Lett. 114B, 287 (1982); W. Bartel *et al.* (JADE Collaboration), Phys. Lett. 114B, 211 (1982); D. Barber *et al.* (MARK J Collaboration), Phys. Rev. Lett. 45, 1904 (1981); R. Brandelik *et al.* (TASSO Collaboration), Phys. Lett. 117B, 365 (1982).